

INSTITUT D'AERONOMIE SPATIALE DE BELGIQUE

3 - Avenue Circulaire  
B - 1180 BRUXELLES

## AERONOMICA ACTA

A - N° 180 - 1977

Stratospheric methane-measurements and predictions

by

M. ACKERMAN, D. FRIMOUT and C. MULLER

BELGISCH INSTITUUT VOOR RUIMTE-AERONOMIE

3 - Ringlaan  
B - 1180 BRUSSEL

## FORWORD

The results described in this note will be presented at the IAGA-IAMAP Assemblies in Seattle (September 1977) and will be published in Pure and Applied Geophysics.

## AVANT-PROPOS

Les résultats décrits dans cette note seront présentés aux Assemblées de l'Association Internationale de Géomagnétisme et d'Aéronomie et de l'Association Internationale de Météorologie et de Physique de l'Atmosphère (Septembre 1977) et seront publiés dans la revue "Pure and Applied Geophysics".

## VOORWOORD

De resultaten beschreven in dit werk, zullen voorgedragen worden ter gelegenheid van de Algemene vergadering van de Internationale Associatie voor Geomagnetisme en Aeronomie en van de Internationale Associatie voor Meteorologie en Atmosferische Fysica (IAGA-IAMAP) in Seattle (september 1977) en zullen gepubliceerd worden in "Pure and Applied Geophysics".

## VORWORT

Die hier beschriebte Ergebnisse wurden zum IAGA-IAMAP Sammlung in Seattle (September 1977) vorgestellt. Dieses Artikel wird in "Pure and Applied Geophysics" veröffentlicht.

# STRATOSPHERIC METHANE-MEASUREMENTS AND PREDICTIONS

by

M. ACKERMAN, D. FRIMOUT and C. MULLER

## *Abstract*

A new determination of stratospheric methane from 22 km to 35 km altitude with implications on the abundance of this constituent at greater heights is presented. Previous measurements some of which showed large discrepancies with currently admitted values have been reinterpreted and brought into agreement. The results are in contradiction according to present theories with the in situ determined CH<sub>4</sub> abundances at the upper edge of the stratosphere.

## *Résumé*

Une nouvelle détermination du méthane stratosphérique de 22 à 35 km d'altitude est présentée avec ses implications sur l'abondance de ce constituant aux altitudes supérieures. Des mesures antérieures, parmi lesquelles d'importants désaccords existaient avec les valeurs couramment admises ont été réinterprétées et mises en accord. Les résultats sont en contradiction selon des théories actuelles avec les abondances déterminées in situ à la limite supérieure de la stratosphère.

### *Samenvatting*

Dit werk bevat een nieuwe bepaling van de stratosferische methaan tussen 22 and 35 km hoogte, samen met de invloed ervan op de dichtheid van dit bestanddeel op grotere hoogten. De vroegere metingen, waarbij belangrijke onenigheid bestond met de algemeen aanvaarde waarden, worden opnieuw geïnterpreteerd en in overeenstemming gebracht. De bekomen resultaten zijn volgens de tegenwoordig aanvaarde theorieën, in tegenspraak met de in situ bepaalde dichtheden, aan de hogere limiet van de stratosfeer.

### *Zusammenfassung*

Eine neue Bestimmung des stratosphärische Methanes zwischen 22 und 35 km Höhe vorgestellt ist mit seine Folge über die  $\text{CH}_4$  Konzentration zum höhere Höhe. Vorherige Beobachtungen sind wiedergestudiert und ein Vergleich zwischen diese geseigt ist. Die Ergebnisse widersprechen die in situ beobachtet Konzentration zum höhere Grens der Stratosphäre zufolge die jetzige Theorië.

## INTRODUCTION

The first determinations of the abundance of  $\text{CH}_4$  in the stratosphere were published by Bains and Heidt [1] in 1966. They showed a decrease of the mixing ratio above the tropopause and were based on in situ sampling with subsequent gas chromatography. Using infrared absorption measurements in the  $7.7 \mu\text{m}$  band, Kyle *et al.* [2] also showed a decrease of the mixing ratio above the tropopause. Ackerman *et al.* [3] indicated also a decrease of concentration with altitude in the stratosphere as well as Cumming and Lowe [4] and Burkert *et al.* [5]. From aircraft borne spectrometer and interferometer data Farmer *et al.* [6] and Lowe and McKinnon [7] showed a decrease of the  $\text{CH}_4$  mixing ratio from low to high latitude in the low stratosphere. The analysis of air samples collected by means of rockets in 1968 and in 1972 have lead to determinations of the methane abundance near the stratopause (Ehhalt *et al.* 1975 [8]).

Since  $\text{CH}_4$  cannot be produced in the stratosphere, its abundance at various altitudes depends on the rate of its chemical destruction and the strength of vertical mixing. This latter property is a basic data for photochemical modeling of the stratosphere. Its knowledge allows for instance the evaluation of the rate of transport of aircraft effluents and other contaminants to the chemically ozone sensitive regions of the upper stratosphere. Several authors (Nicolet and Peetermans [9], Wofsy and McElroy [10], Hunten [11]) have attempted to deduce values of the vertical transport parameters using the available methane data. Chang [12] has analysed the various values and shown that the improvement of experimental data can reduce the present uncertainty and consequently the uncertainties in the models and in their predictions.

The present work is an attempt to reduce the uncertainty. It consists of the determination of the abundance of  $\text{CH}_4$  from 22 to 40 km using high resolution infrared absorption spectroscopic measurements interpreted on the basis of the presently available laboratory spectroscopic data followed by a discussion of other results and of theoretical evaluations.

## INSTRUMENTATION AND OBSERVATION

A 60 cm focal length grille spectrometer was flown on October 2, 1975 from the CNES range in Aire sur l'Adour to measure the vertical distribution of HCl in the stratosphere (Ackerman *et al.* [13]). Observations of the solar spectrum from an altitude of 35 km took place in the wavenumbers range from  $2916 \text{ cm}^{-1}$  to  $2970 \text{ cm}^{-1}$  which includes the  $P_5$  to  $P_9$  multiplets of the  $3.3 \mu\text{m}$  band of  $\text{CH}_4$  (fig. 1). The range of solar zenith angles from  $80^\circ.5$  to  $95^\circ.5$  was covered at  $43^\circ\text{N}$  and  $2^\circ\text{E}$ . The methane absorptions shown in figure 1 were always present in the spectra. Those due to  $P_9$  are perturbed by solar absorption features and are not considered in this work. The measured equivalent widths of the multiplets are shown in figure 2 versus elevation angles for observation above the horizontal and listed in table 1 versus grazing altitude of the solar rays for observations below the horizontal.

## INTERPRETATION OF THE DATA

### *a) Observations above the horizontal*

Values of the number density and of the scale height have been assumed, to compute equivalent widths by dividing the atmosphere in layers of 1 km thickness to take into account the change of path length, pressure and temperature as a function of height in the successive layers above float altitudes according to the earth geometry and to the mid-latitude Spring- Fall model of the US Standard Atmosphere supplement, 1966. A Voigt profile has been introduced in the computation for each line of the multiplets of which the spectroscopic data taken from Toth *et al.* [14] and from MacClatchey *et al.* [15] are given in Table 2. The change of equivalent width with solar elevation angle for the four multiplets has been computed and is shown in figure 2 with the data. The shaded curves marked I represent the equivalent widths that should be observed if the number density at 35 km, was equal to  $(1.46 \pm 0.12) \times 10^{11} \text{ cm}^{-3}$  and if the scale height was equal to 4.54 km. These values correspond to the mixing ratio values published by Ehhalt *et al.* [8] and used in models to evaluate the strength of the vertical transport of methane. The range of values taken for the number density at 35 km is obtained from the mixing ratio value published by

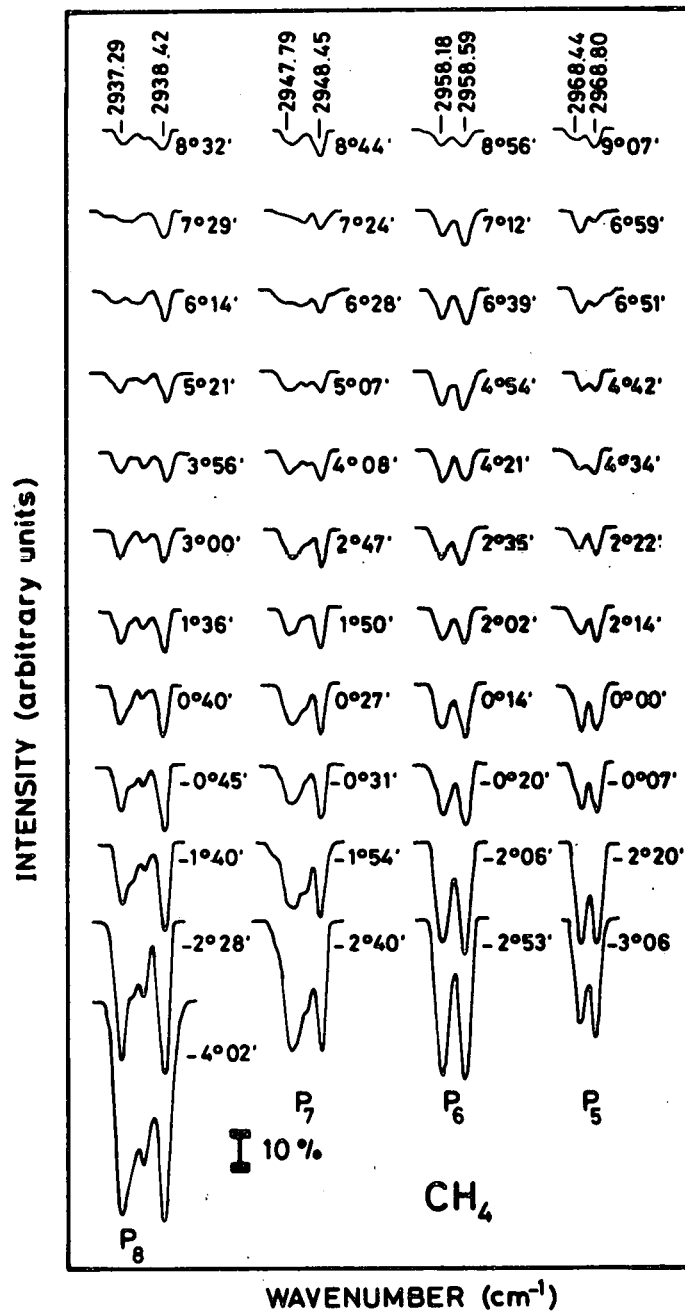


Fig. 1.- Portions of absorption spectra recorded on October 2, 1975, from 35 km altitude at 43°N and 2°E in the 3.3 μm CH<sub>4</sub> band. Multiplets P<sub>5</sub> to P<sub>8</sub> are shown with some identification wavenumbers in cm<sup>-1</sup>. The angular values shown on the righthandside of each portion of spectrum are solar elevation and solar depression angles for positive and negative values respectively.

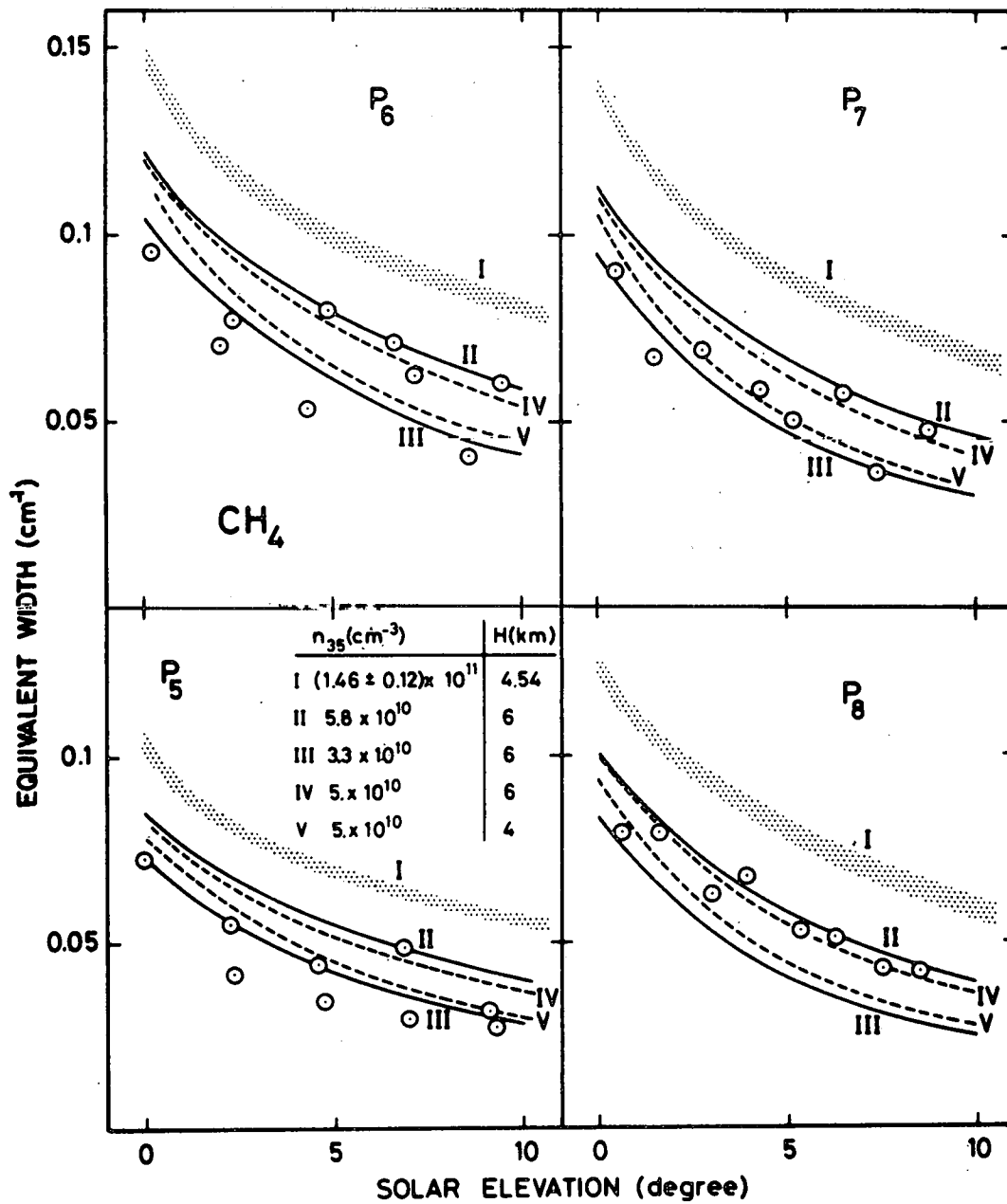


Fig. 2.- Equivalent width versus solar elevation angle. The circles represent the measurements. The shaded curves correspond to the mixing ratio values represented by the solid broken curve of figure 4. The other curves correspond to the CH<sub>4</sub> number densities at 35 km [ $n_{35}(\text{cm}^{-3})$ ] and to the scale heights above this altitude H(km) indicated on the figure.



TABLE 1.- Equivalent widths in  $\text{cm}^{-1}$  of the  $3.3 \mu\text{m}$  P branch multiplets of  $\text{CH}_4$  versus minimum altitudes,  $z$ , reached by the solar rays.

$z(\text{km})$	$P_5$	$P_6$	$P_7$	$P_8$
35	$7.1 \times 10^{-2}$	$1.06 \times 10^{-1}$	$6.8 \times 10^{-2}$	$8.5 \times 10^{-2}$
33	$1.16 \times 10^{-1}$	$1.64 \times 10^{-1}$	$1.33 \times 10^{-1}$	$1.10 \times 10^{-1}$
31	$1.53 \times 10^{-1}$	$2.19 \times 10^{-1}$	$2.00 \times 10^{-1}$	$1.52 \times 10^{-1}$
29	$2.11 \times 10^{-1}$	$2.76 \times 10^{-1}$	$2.75 \times 10^{-1}$	$2.10 \times 10^{-1}$
27			$3.70 \times 10^{-1}$	$2.82 \times 10^{-1}$
25				$3.66 \times 10^{-1}$
23				$4.91 \times 10^{-1}$
21				$6.41 \times 10^{-1}$

TABLE 2.- Line positions  $\lambda$ , integrated absorption cross sections, S, full width at half height W and ground level Energies E for the CH<sub>4</sub> multiplets considered in the treatment of the data .

	$\lambda(\text{cm}^{-1})$	S ( $\text{cm}^2.\text{cm}^{-1}$ ) 297°K	W ( $\text{cm}^{-1}$ )	E ( $\text{cm}^{-1}$ )
P <sub>5</sub>	2968.885	7.06 x 10 <sup>-20</sup>	0.122	157
	2968.770	1.27 x 10 <sup>-21</sup>	0.094	157
	2968.738	7.06 x 10 <sup>-20</sup>	0.122	157
	2968.473	7.06 x 10 <sup>-20</sup>	0.122	157
	2968.404	7.06 x 10 <sup>-20</sup>	0.122	157
P <sub>6</sub>	2958.683	4.40 x 10 <sup>-20</sup>	0.114	219
	2958.651	6.58 x 10 <sup>-20</sup>	0.118	219
	2958.537	1.10 x 10 <sup>-19</sup>	0.102	219
	2958.233	6.62 x 10 <sup>-20</sup>	0.118	219
	2958.120	6.42 x 10 <sup>-20</sup>	0.118	219
	2958.017	1.12 x 10 <sup>-19</sup>	0.102	219
P <sub>7</sub>	2948.478	5.13 x 10 <sup>-20</sup>	0.114	293
	2948.421	5.00 x 10 <sup>-20</sup>	0.114	293
	2948.130	1.13 x 10 <sup>-21</sup>	0.102	219
	2948.107	8.47 x 10 <sup>-20</sup>	0.114	293
	2947.912	4.88 x 10 <sup>-20</sup>	0.114	293
	2947.810	3.28 x 10 <sup>-20</sup>	0.114	293
	2947.700	1.13 x 10 <sup>-21</sup>	0.102	219
	2947.668	5.00 x 10 <sup>-20</sup>	0.114	293
P <sub>8</sub>	2938.248	6.46 x 10 <sup>-20</sup>	0.110	376
	2938.206	3.88 x 10 <sup>-20</sup>	0.110	376
	2938.206	2.59 x 10 <sup>-20</sup>	0.110	376
	2937.769	3.88 x 10 <sup>-20</sup>	0.110	376
	2937.494	3.88 x 10 <sup>-20</sup>	0.110	376
	2937.307	2.70 x 10 <sup>-20</sup>	0.110	376
	2937.234	3.95 x 10 <sup>-20</sup>	0.110	376

Ehhalt *et al.* [8] and from the extreme values of total number densities given in the US Standard Atmosphere Supplement, 1966. The computed equivalent widths do not fit the experimental data points. The computation has then been made for various sets of  $n_{35}$  and scale heights. Changing the scale height values from 4.5 km to 6.0 km has the most appreciable effect on the change of equivalent width with elevation angle at small angle. The scatter of the measured values does not allow to make a clear choice. However there is a tendency indicating that the scale height above 35 km is at least over a few kilometers altitude closer to 6 km so that the values corresponding to curves II and III of figure 2 have been represented in figures 3 and 4 where envelopes are shown at and above 35 km for the  $\text{CH}_4$  number densities and mixing ratios respectively with the results of other investigators.

#### ***b) Observations below the horizon***

The amount of methane above 35 km has been taken into account by choosing a scale height equal to 6 km and a number density of  $4.5 \times 10^{10}$  at 35 km, both values being the result of the preceding section. The number densities below float altitude in successive layers of 2 km thickness have been determined from the equivalent widths listed in table 1. The same atmospheric model and spectroscopic data as in the previous sections have been introduced in the computation. The results are shown in figures 3 and 4 as number densities and volume mixing ratios respectively.

#### **COMPARISON WITH OTHER RESULTS**

For sets of spectroscopic data are available about stratospheric methane. They cover a period of 10 years since the measurements published by Kyle *et al.* [2] were performed in December 1967 at 33° North. The  $\nu_4$  band, from  $1299 \text{ cm}^{-1}$  to  $1306 \text{ cm}^{-1}$ , was observed in absorption during a balloon ascent for solar elevation angles from 31° to 5°. The authors give all information required to reinterpret their observations. After ten years the quality of spectroscopic parameters has greatly improved. This situation justifies a new analysis.

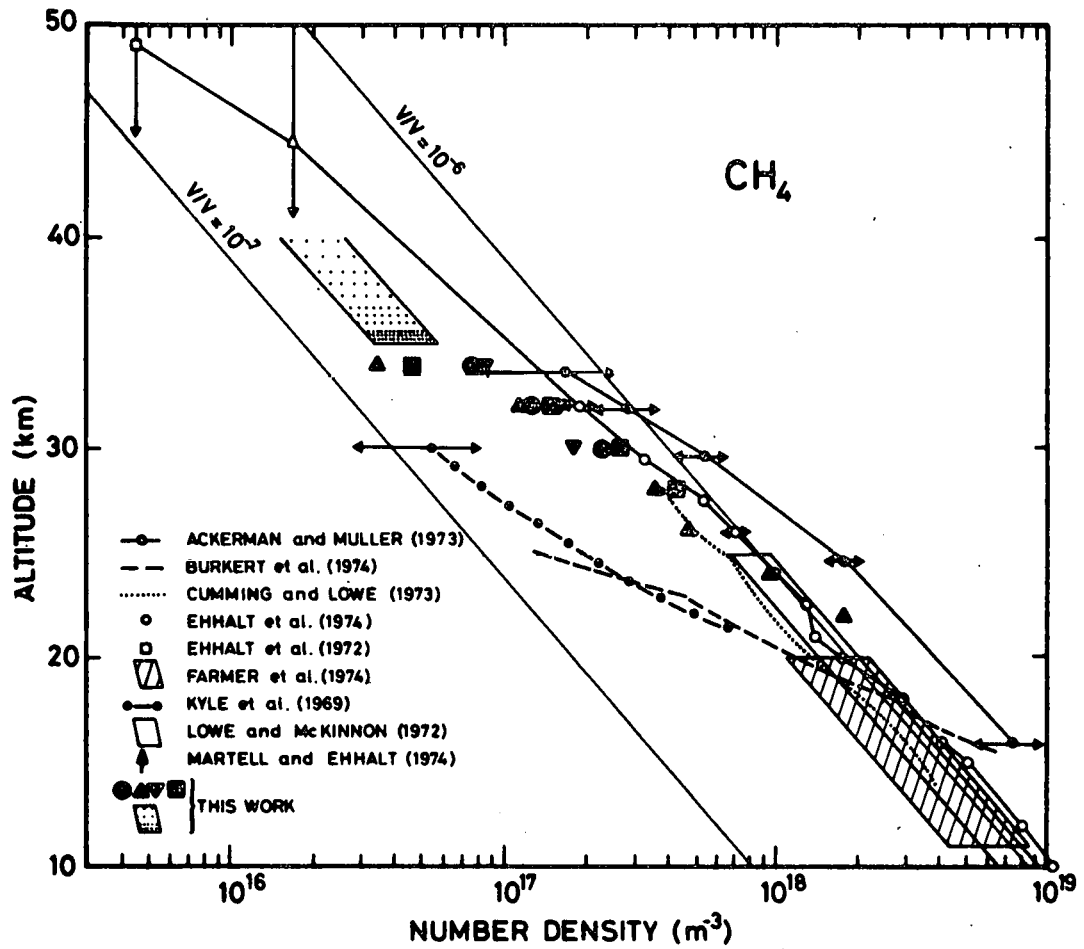


Fig. 3.- Methane number densities as published by various groups of authors and reported by Hard [19] with the values deduced from the observations reported in the present work. The arrowed vertical lines centered on the values between 40 and 50 km indicate the altitude range of vertical rocket sampling.

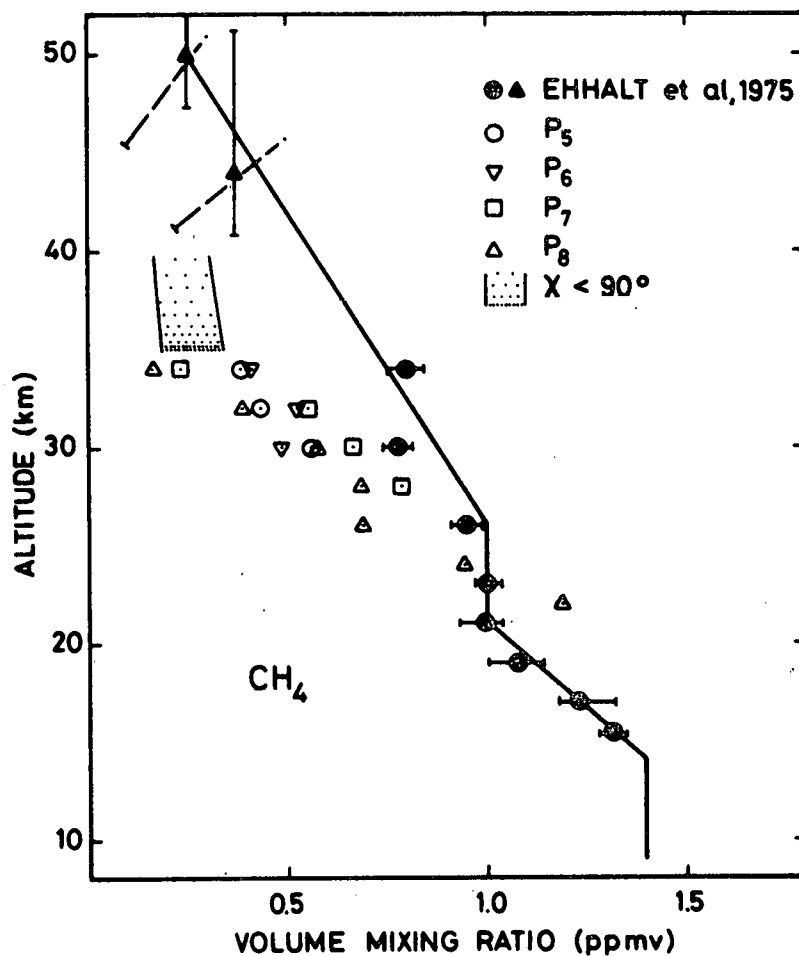


Fig. 4.- Methane mixing ratio as a function of altitude. The presently reported observations are shown with the values from Ehhalt *et al.* [8]. Tilted dashed bars are shown with the rocket determinations in order to keep this figure consistent with the previous one (figure 3).

This has been made, following the method already described previously on the basis of the spectroscopic data of Mc Clatchey *et al.* [15] listed in table 3. However, nitrous oxide absorbs in the region from  $1299.1 \text{ cm}^{-1}$  to  $1307 \text{ cm}^{-1}$  which is considered. For this reason, the analysis has been limited to the balloon float period. A number density of  $\text{N}_2\text{O}$  at 28 km equal to  $6 \times 10^{10} \text{ cm}^{-3}$  has been assumed with a scale height of 3.7 km leading to a maximum contribution to the equivalent width equal to  $0.1 \text{ cm}^{-1}$ . The observations are then, as shown in figure 5, well represented if methane number density and scale height are respectively taken equal to  $2 \times 10^{11} \text{ cm}^{-3}$  and 4 km. This represents an increase by a factor of almost 4 of the original values published by Kyle *et al.* [2] bringing them in agreement with others.

Enough flight data were given by Cumming and Lowe [4] in their publication to reinterpret their observation made at  $47^\circ \text{N}$  in August 1965 and at 28 km float altitude. A computation was made using the now available spectroscopic data on the components of the  $\text{R}_5$  multiplet of the  $3.3 \mu\text{m } \nu_3$  band. As shown in figure 6, a  $\text{CH}_4$  number density and a scale height equal to  $3 \times 10^{11} \text{ cm}^{-3}$  and 4.5 km respectively at 28 km, fit the data points and are in good agreement with the original result of the authors.

In the spectra obtained by Ackerman *et al.* [3] in October 1971 at  $43^\circ \text{N}$ , the Q branch of the  $3.3 \mu\text{m}$  band of  $\text{CH}_4$  is the most prominent feature which at the time of the publication could not be analysed due to the lack of availability of a powerful enough computer. This has now partly been done. The equivalent width equal to  $0.8 \pm 0.1 \text{ cm}^{-1}$  observed at 35 km for a zenith angle equal to  $90^\circ$  is represented by a  $\text{CH}_4$  number density equal to  $(4.5 \pm 1.5) \times 10^{10} \text{ cm}^{-3}$  associated with a scale height equal to 4 km. This brings downward the values published in 1972 which have always appeared to be systematically to high.

## DISCUSSION

Four sets of data obtained at various latitudes and seasons are now available at 30 km altitude for a period of ten years. The values derived on the basis of a consistent set of

TABLE 3.- Spectroscopic data used for the  $\nu_4$ CH<sub>4</sub> band. The symbols have the same meaning as in Table 2.

$\lambda$ (cm <sup>-1</sup> )	$S_{297}$ (cm <sup>2</sup> .cm <sup>-1</sup> )	W (cm <sup>-1</sup> )	E (cm <sup>-1</sup> )
1299.638	2.35 x 10 <sup>-20</sup>	0.112	293.10
1299.678	1.71 x 10 <sup>-21</sup>	0.098	950.27
1299.903	2.35 x 10 <sup>-20</sup>	0.112	293.11
1299.903	8.32 x 10 <sup>-21</sup>	0.104	575.14
1300.282	6.21 x 10 <sup>-21</sup>	0.130	10.48
1300.467	8.33 x 10 <sup>-21</sup>	0.104	575.23
1300.467	1.71 x 10 <sup>-21</sup>	0.098	950.30
1300.748	2.99 x 10 <sup>-22</sup>	0.096	1251.7
1301.208	2.05 x 10 <sup>-21</sup>	0.100	814.61
1301.290	4.48 x 10 <sup>-22</sup>	0.096	1251.8
1301.371	1.94 x 10 <sup>-20</sup>	0.112	219.90
1301.500	8.37 x 10 <sup>-21</sup>	0.106	470.77
1301.550	2.92 x 10 <sup>-20</sup>	0.116	219.92
1301.550	3.07 x 10 <sup>-21</sup>	0.100	814.97
1301.825	1.25 x 10 <sup>-20</sup>	0.106	470.78
1302.040	4.86 x 10 <sup>-20</sup>	0.100	219.90
1302.040	9.01 x 10 <sup>-22</sup>	0.098	1095.6
1302.451	5.21 x 10 <sup>-21</sup>	0.102	689.93
1302.774	1.78 x 10 <sup>-20</sup>	0.110	376.80
1302.774	3.35 x 10 <sup>-20</sup>	0.120	157.11
1302.774	2.85 x 10 <sup>-21</sup>	0.098	950.35
1302.945	2.09 x 10 <sup>-20</sup>	0.106	470.81
1303.198	1.39 x 10 <sup>-20</sup>	0.104	575.19
1303.290	3.67 x 10 <sup>-22</sup>	0.122	000.00
1303.373	3.35 x 10 <sup>-20</sup>	0.120	157.12
1303.567	3.93 x 10 <sup>-20</sup>	0.112	293.13
1303.709	5.13 x 10 <sup>-21</sup>	0.100	815.05
1303.709	5.90 x 10 <sup>-20</sup>	0.092	104.77
1303.709	7.49 x 10 <sup>-22</sup>	0.096	1252.0
1303.951	1.78 x 10 <sup>-20</sup>	0.110	376.71
1304.223	3.54 x 10 <sup>-20</sup>	0.124	104.77
1304.332	5.22 x 10 <sup>-21</sup>	0.102	689.99
1304.463	2.36 x 10 <sup>-20</sup>	0.112	293.15
1304.602	9.03 x 10 <sup>-22</sup>	0.098	1095.6

TABLE 3.- continued.

$\lambda$ (cm <sup>-1</sup> )	$S_{297}$ (cm <sup>2</sup> .cm <sup>-1</sup> )	W (cm <sup>-1</sup> )	E (cm <sup>-1</sup> )
1304.602	2.36 x 10 <sup>-20</sup>	0.108	104.77
1304.602	8.35 x 10 <sup>-21</sup>	0.104	575.15
1304.847	1.71 x 10 <sup>-21</sup>	0.098	950.45
1304.847	3.38 x 10 <sup>-20</sup>	0.124	62.87
1305.002	2.92 x 10 <sup>-20</sup>	0.116	219.90
1305.002	1.57 x 10 <sup>-20</sup>	0.112	293.15
1305.092	1.26 x 10 <sup>-20</sup>	0.106	470.83
1305.286	3.08 x 10 <sup>-21</sup>	0.100	814.83
1305.286	5.57 x 10 <sup>-21</sup>	0.104	575.02
1305.413	3.38 x 10 <sup>-20</sup>	0.124	62.87
1305.454	1.88 x 10 <sup>-20</sup>	0.102	31.43
1305.454	4.50 x 10 <sup>-22</sup>	0.096	1252.0
1305.563	2.24 x 10 <sup>-20</sup>	0.120	157.13
1305.563	1.14 x 10 <sup>-21</sup>	0.098	950.47
1305.635	2.92 x 10 <sup>-20</sup>	0.116	219.93
1305.635	1.19 x 10 <sup>-20</sup>	0.110	376.71
1305.688	2.81 x 10 <sup>-20</sup>	0.130	31.44
1305.809	3.48 x 10 <sup>-21</sup>	0.102	690.01
1305.809	1.87 x 10 <sup>-20</sup>	0.130	10.48
1305.809	1.26 x 10 <sup>-20</sup>	0.106	470.84
1305.905	3.36 x 10 <sup>-20</sup>	0.120	157.13
1305.989	3.55 x 10 <sup>-20</sup>	0.124	104.77
1305.989	6.03 x 10 <sup>-22</sup>	0.098	1095.2
1305.989	3.08 x 10 <sup>-21</sup>	0.100	814.61
1306.021	1.78 x 10 <sup>-20</sup>	0.110	376.76
1306.106	2.36 x 10 <sup>-20</sup>	0.112	296.16
1306.106	5.64 x 10 <sup>-20</sup>	0.112	62.87
1306.254	4.88 x 10 <sup>-20</sup>	0.100	219.93
1306.254	4.50 x 10 <sup>-22</sup>	0.096	1252.0
1306.254	8.36 x 10 <sup>-21</sup>	0.104	575.02
1306.254	5.23 x 10 <sup>-21</sup>	0.102	690.02
1306.428	2.10 x 10 <sup>-20</sup>	0.106	470.85
1306.428	1.72 x 10 <sup>-21</sup>	0.098	950.49
1306.627	9.04 x 10 <sup>-22</sup>	0.098	1095.2
1306.627	5.14 x 10 <sup>-21</sup>	0.100	814.61
1306.832	7.51 x 10 <sup>-22</sup>	0.096	1252.0



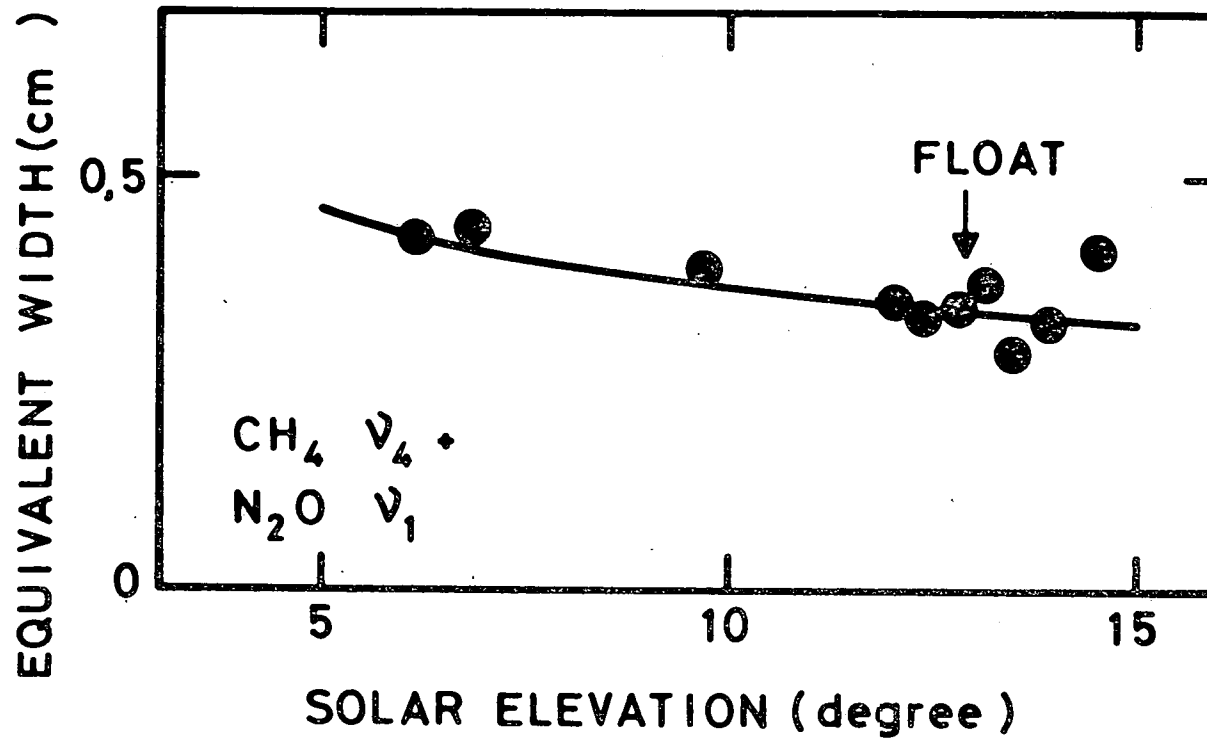


Fig. 5.- Equivalent width observed at balloon float altitude by Kyle *et al.* [2] before sunset versus solar elevation angle. The curve corresponds to a methane number density at 30 km equal to  $2 \times 10^{11} \text{ cm}^{-3}$  associated with a scale height of 4 km. The N<sub>2</sub>O absorption of  $0.1 \text{ cm}^{-1}$  equivalent widths has been taken into account, corresponding to an N<sub>2</sub>O number density at 30 km equal to  $6 \times 10^{10} \text{ cm}^{-3}$  associated with a scale height of 3.7 km.

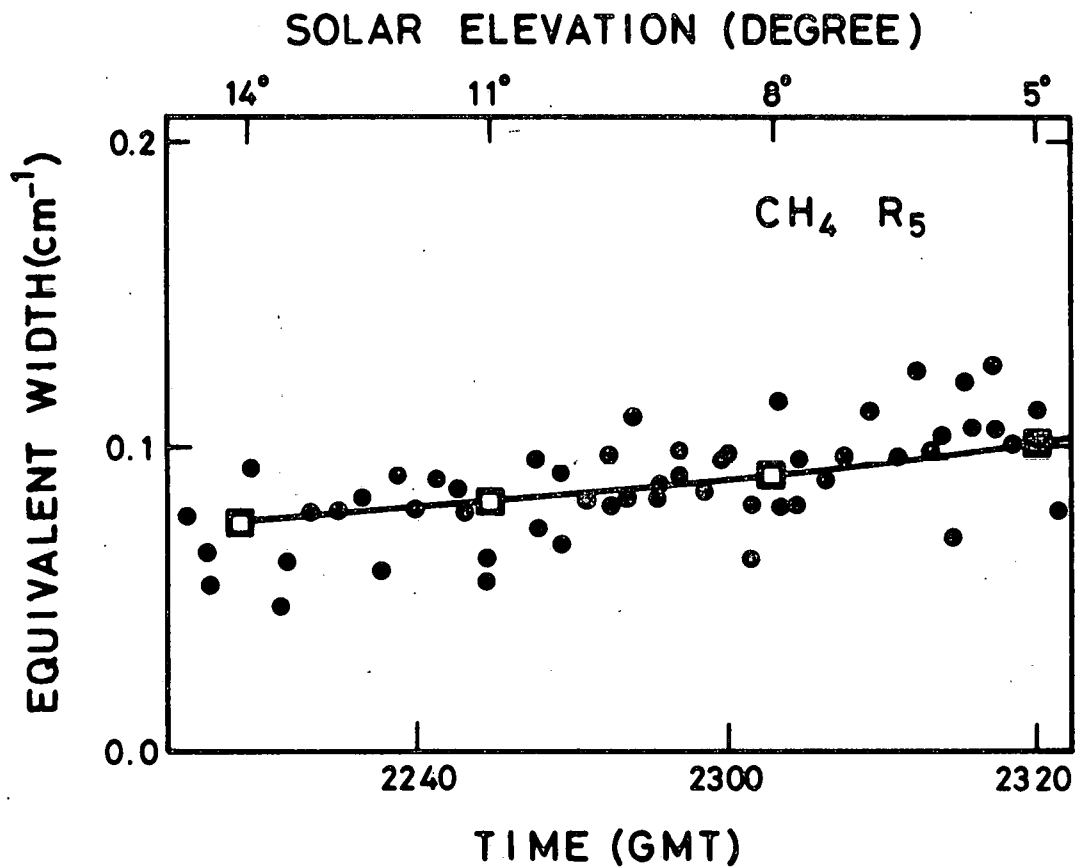
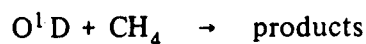


Fig. 6.- Equivalent width due to the R<sub>5</sub>CH<sub>4</sub> multiplet observed by Cumming and Lowe [4] versus time during the float period of the gondola. The circles and the solid line are from the original publication, The squares correspond to the reinterpretation with a CH<sub>4</sub> number density at 28 km altitude equal to  $3 \times 10^{11}$  associated with a scale height equal to 4.5 km, both being in good agreement with the original interpretation.

spectroscopic parameters are listed in table 4 with in situ sampling results. No significance in terms of geographic, time or season variability can be attributed to the differences appearing between the various values since the uncertainties are most probably larger than these differences. Methane number density at 30 km appears to be very stable within experimental error limits.

An envelope of the new methane mixing ratios presented here is shown in figure 7 with values predicted by Chang [12] on the basis of a unified chemical scheme with different vertical distributions of vertical transport coefficients. Curve B appears to fit the experimental data in the worst fashion while curves A and C bring the best agreement within the uncertainty limits. Values of the vertical transport coefficient have been evaluated on the basis of the number densities of  $\text{CH}_4$ , OH and  $\text{O}^1\text{D}$  shown in table 5. The rate constants for the reactions



and



published by Nicolet [20], namely  $3 \times 10^{-3} \text{ cm}^3 \text{ sec}^{-1}$  and  $3.5 \times 10^{-12} e^{-1800/T} \text{ cm}^{-3} \text{ sec}^{-1}$  respectively, have been used.

The uncertainty shown on figure 8 in the altitude range around 25 km is the consequence of the rather abrupt change of methane scale height in the middle stratosphere.

Low stratospheric methane abundances will have various consequences on model calculations of other species. They will have the effect of reducing the HCl/ClO ratio, as an example.

TABLE 4.- Methane number densities at 30 km altitude.

CH <sub>4</sub> number density (cm <sup>-3</sup> )	Time	Latitude	Ref.
1.9 x 10 <sup>11</sup>	August 1965	47° N	[4]
2 x 10 <sup>11</sup>	December 1967	33° N	[2]
2 x 10 <sup>11</sup>	October 1971	43° N	[3]
2.2 x 10 <sup>11</sup>	October 1975	43° N	This work
3 x 10 <sup>11</sup>	--	32° N	[8]

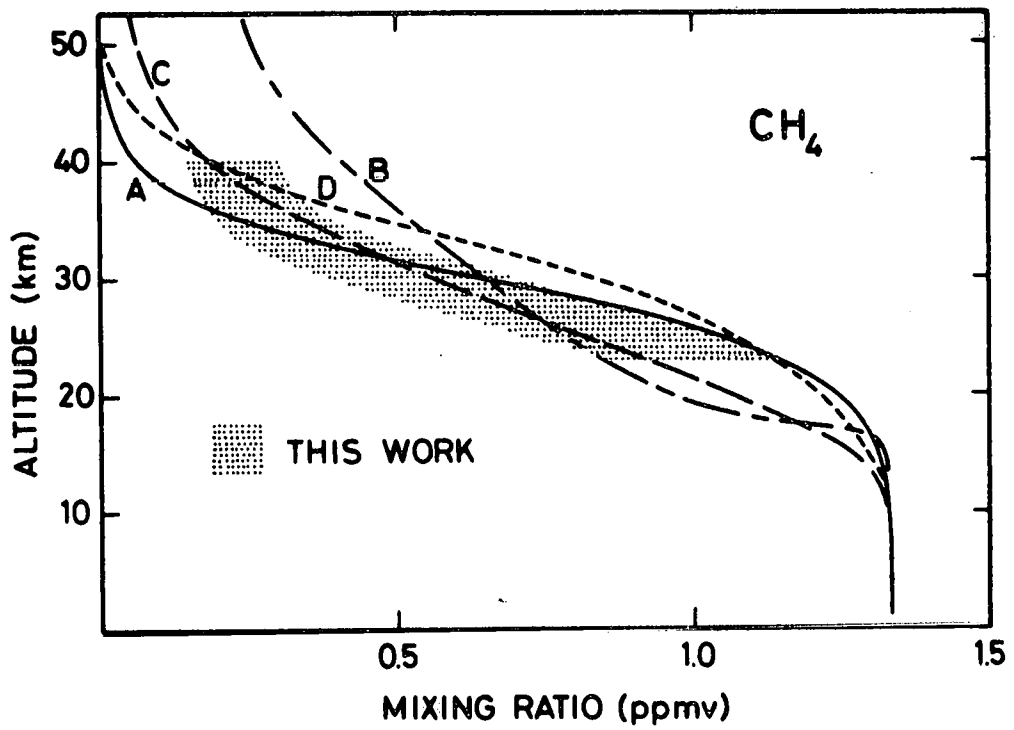


Fig. 7.- Vertical distributions of the CH<sub>4</sub> volume mixing ratio computed by Chang [12].  
The envelope represents the new observations presented here.

TABLE 5.- Data used in conjunction with the mid-latitude Spring-Fall model of U.S. Standard Atmosphere supplement, 1966, to evaluate the vertical transport coefficient, K.

Altitude km	$n(O^1D)$ $cm^{-3}$	$n(OH)$ $cm^{-3}$	$n(CH_4)$ $cm^{-3}$
12	$2.4 \times 10^{-2}$	$2.1 \times 10^5$	$9.09 \times 10^{12}$
14	6.2	2.3	6.49
16	$1.5 \times 10^{-1}$	2.5	4.43
18	3.4	3.0	2.96
20	9.0	3.6	1.96
22	$1.6 \times 10^0$	4.4	1.35
24	3.3	5.5	$9.46 \times 10^{11}$
26	6.5	7.0	6.27
28	$1.2 \times 10^1$	9.0	3.80
30	2.0	$1.4 \times 10^6$	2.15
32	3.1	1.7	1.21
34	4.8	2.5	$7.00 \times 10^{10}$
36	6.8	3.8	4.23
38	9.2	5.4	2.69
40	$1.4 \times 10^2$	7.0	1.91
42	1.6	8.4	1.18
44	2.0	9.6	$6.58 \times 10^9$
46	2.6	$1.2 \times 10^7$	2.49

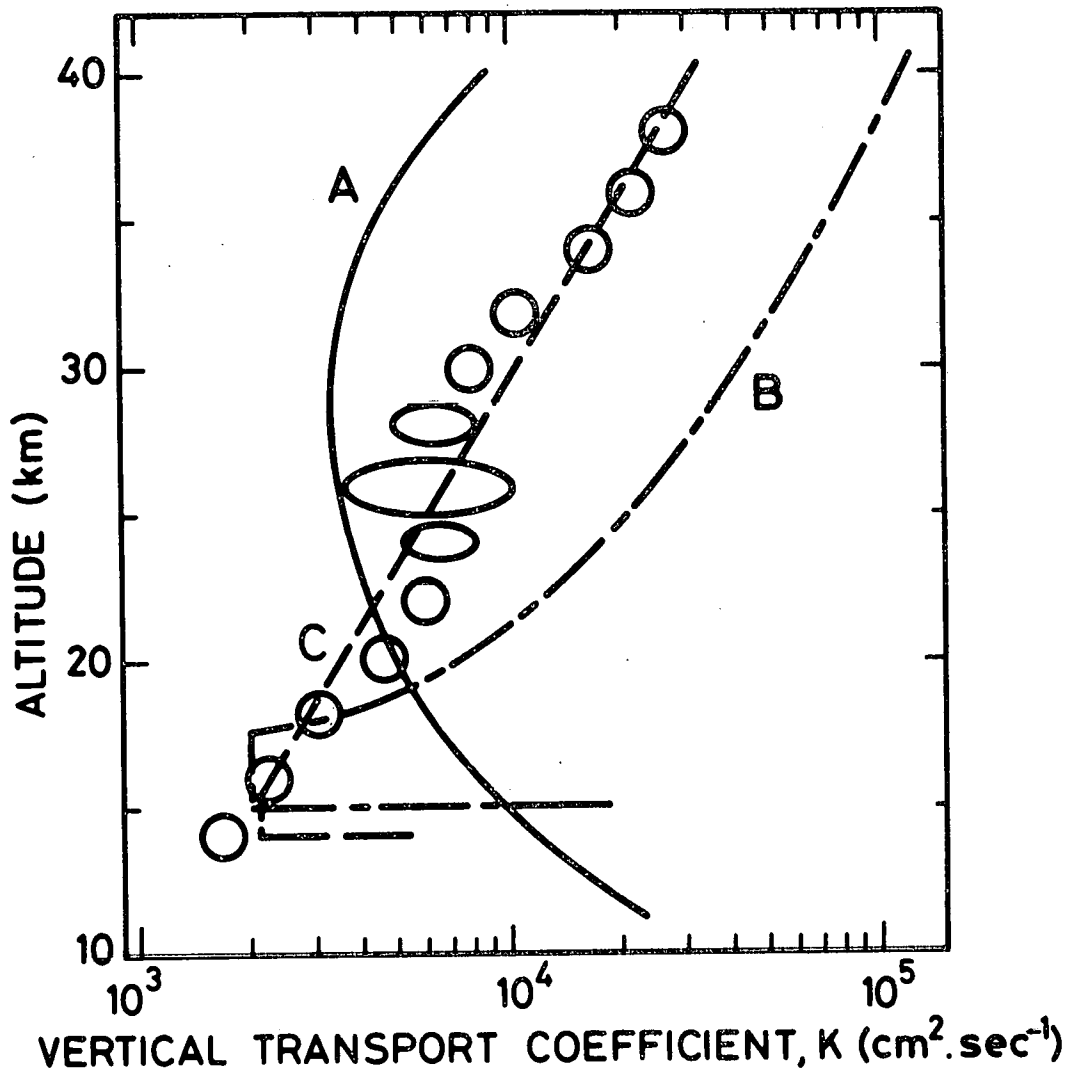


Fig. 8.- Vertical distribution of vertical transport coefficient computed on the basis of the data presented in table 5 (circles). Curves A, B and C are from references [12], [10] and [11] respectively. The uncertainty represented around 25 km results from the change of CH<sub>4</sub> scale height at these altitudes.

## *CONCLUSION*

New stratospheric methane measurements have been presented with previous measurements reinterpreted on the basis of a consistent set of spectroscopic parameters. Discrepancies with values obtained at the upper edge of the stratosphere by means of in situ sampling calls for new measurements, particularly at those altitudes.

## *ACKNOWLEDGEMENT*

Thanks are due to M. Rosseeuw for computer programming.



## REFERENCES

- [1] A.E. BAINBRIDGE and L.E. HEIDT, Measurements of methane in the troposphere and lower stratosphere. *Tellus*, 18 (1966), 221-114.
- [2] T.G. KYLE, D.G. MURCRAY, F.H. MURCRAY and W.J. WILLIAMS, Abundance of methane in the atmosphere above 20 kilometers. *J. Geophys. Res.*, 74 (1969), 3421-3425.
- [3] M. ACKERMAN, D. FRIMOUT, C. LIPPENS et C. MULLER, Détermination de la distribution verticale du méthane stratosphérique par spectrométrie infrarouge en ballon. *Bull. Acad. Roy. Belgique, Cl. Sc.*, 55 (1972), 493-501.
- [4] C. CUMMING and R.P. LOWE, Balloon-borne spectroscopic measurement of stratospheric methane. *J. Geophys. Res.*, 78 (1973), 5259-5264.
- [5] P. BURKERT, D. RABUS, H.J. BOLLE, Stratospheric water vapor and methane profiles. Proc. Int. Conf. on Struct., Compos. and Gen. Circ. of the Upper and Lower Atmos. and Poss. Anthrop. Pert. Vol 1 (1974), 267-274.
- [6] C.B. FARMER, O.F. RAPER, R.A. TOTH, R.A. SCHINDLER, Recent results of aircraft infrared observations of the stratosphere. Proc. Third Conf. on the Climatic Impact Assessment Program, Rep. No. DOT-TSC-OST-74-15, U.S. Dept. of Transport (1974), 234-245.
- [7] R.P. LOWE and D. MCKINNON, Measurements of stratospheric methane over north America. *Can. J. Phys.*, 50 (1972), 668-673.
- [8] D.H. EHHALT, L.E. HEIDT, R.H. LUEB, W. POLLOCK, The vertical distribution of trace gases in the stratosphere. *Pageoph.* 113 (1975), 389-402.
- [9] M. NICOLET and W. PEETERMANS, On the vertical distribution of carbon monoxide and methane in the stratosphere. *Pageoph.* 106-108 (1973), 1400-1416.
- [10] S.C. WOFSY and M.B. McELROY, On vertical mixing in the upper stratosphere and lower mesosphere. *J. Geophys. Res.*, 78 (1973), 2619-2624.
- [11] D.M. HUNTEN, The philosophy of one-dimensional modeling. Proc. Fourth Conf. on the Climatic Impact Assessment Program, Rep. No. DOT-TSC-OST-75-38, U.S. Dept. of Transport (1975), 147-155.
- [12] J.S. CHANG, Uncertainties in the validation of parameterized transport in 1 D models of the stratosphere. Proc. Fourth Conf. on the Climatic Impact Assessment Program

- Rep. No. DOT-TSC-OST-75-38, U.S. Dept. of Transport. (1975), 175-182.
- [13] M. ACKERMAN, D. FRIMOUT, A. GIRARD, M. GOTTIGNIES, C. MULLER, Stratospheric HCl from infrared spectra. *G.R.L.* 3 (1976), 81-83.
- [14] R.A. TOTH, L.R. BROWN, R.A. HUNT, Line positions and strengths of methane in the 2862 to 3000  $\text{cm}^{-1}$  Region. *J. Mol. Spectry*, in press.
- [15] R.A. McCLATCHEY, W.S. BENEDICT, S.A. CLOUGH, D.E. BURCH, R.F. CALFEE, K. FOX, L.S. ROTHMAN, J.S. GARING, AFCRL atmospheric absorption line parameters compilation. AFCRL-TR-73-0096, Environmental Research Papers No. 434, L.G. Hanscom Field, Bedford, Mass. 01730 (1973).
- [16] E.A. MARTELL and D.H. EHHALT, Hydrogen and carbon compounds in the upper stratosphere and lower mesosphere. Proc. Int. Conf. on Struct., Compos. and Gen. Circ. of the Upper and Lower Atmos. and Possible Anthropogenic Perturbations, vol. 1 (1974), 223-229.
- [17] D.H. EHHALT, L.E. HEIDT, E.A. MARTELL, The concentration of atmospheric methane between 44 and 62 kilometers altitude. *J. Geophys. Res.*, 77 (1972), 2193-2196.
- [18] D.H. EHHALT, L.E. HEIDT, R.H. LUEB, N. ROPER, Vertical profiles of  $\text{CH}_4$ ,  $\text{H}_2$ ,  $\text{CO}$ ,  $\text{N}_2\text{O}$  and  $\text{CO}_2$  in the stratosphere, Proc. Third Conf. on the Climatic Impact Assessment Program, Rep. No. DOT-TSC-OST-74-15, U.S. Depart. of Transport. (1974) 153-160.
- [19] T.M. HARD, Summary of recent report of stratospheric trace-gas profiles, The natural stratosphere of 1974, CIAP Monograph 1, Depart. of Transport, U.S., DOT-TST-75-51. (1975), 3-162-3-170.
- [20] M. NICOLET, Stratospheric Ozone : an introduction to its study. *Rev. Geophys. Space Phys.*, 13 (1975), 593-636.

- 111 - ACKERMAN, M. and P. SIMON, Rocket measurement of solar fluxes at 1216 Å, 1450 Å and 1710 Å, 1972.
- 112 - CIESLIK, S. and M. NICOLET, The aeronomic dissociation of nitric oxide, 1973.
- 113 - BRASSEUR, G. and M. NICOLET, Chemospheric processes of nitric oxide in the mesosphere and stratosphere, 1973.
- 114 - CIESLIK, S. et C. MULLER, Absorption raie par raie dans la bande fondamentale infrarouge du monoxyde d'azote, 1973.
- 115 - LEMAIRE, J. and M. SCHERER, Kinetic models of the solar and polar winds, 1973.
- 116 - NICOLET, M., La biosphère au service de l'atmosphère, 1973.
- 117 - BIAUME, F., Nitric acid vapor absorption cross section spectrum and its photodissociation in the stratosphere, 1973.
- 118 - BRASSEUR, G., Chemical kinetic in the stratosphere, 1973.
- 119 - KOCKARTS, G., Helium in the terrestrial atmosphere, 1973.
- 120 - ACKERMAN, M., J.C. FONTANELLA, D. FRIMOUT, A. GIRARD, L. GRAMONT, N. LOUISNARD, C. MULLER and D. NEVEJANS, Recent stratospheric spectra of NO and NO<sub>2</sub>, 1973.
- 121 - NICOLET, M., An overview of aeronomic processes in the stratosphere and mesosphere, 1973.
- 122 - LEMAIRE, J., The "Roche-Limit" of ionospheric plasma and the formation of the plasmopause, 1973.
- 123 - SIMON, P., Balloon measurements of solar fluxes between 1960 Å and 2300 Å, 1974.
- 124 - ARIJS, E., Effusion of ions through small holes, 1974.
- 125 - NICOLET, M., Aëronomic, 1974.
- 126 - SIMON, P., Observation de l'absorption du rayonnement ultraviolet solaire par ballons stratosphériques, 1974.
- 127 - VERCHEVAL, J., Contribution à l'étude de l'atmosphère terrestre supérieure à partir de l'analyse orbitale des satellites, 1973.
- 128 - LEMAIRE, J. and M. SCHERER, Exospheric models of the topside ionosphere, 1974.
- 129 - ACKERMAN, M., Stratospheric water vapor from high resolution infrared spectra, 1974.
- 130 - ROTH, M., Generalized invariant for a charged particle interacting with a linearly polarized hydromagnetic plane wave, 1974.
- 131 - BOLIN, R.C., D. FRIMOUT and C.F. LILLIE, Absolute flux measurements in the rocket ultraviolet, 1974.
- 132 - MAIGNAN, M. et C. MULLER, Méthodes de calcul de spectres stratosphériques d'absorption infrarouge, 1974.
- 133 - ACKERMAN, M., J.C. FONTANELLA, D. FRIMOUT, A. GIRARD, N. LOUISNARD and C. MULLER, Simultaneous measurements of NO and NO<sub>2</sub> in the stratosphere, 1974.
- 134 - NICOLET, M., On the production of nitric oxide by cosmic rays in the mesosphere and stratosphere, 1974.
- 135 - LEMAIRE, J. and M. SCHERER, Ionosphere-plasmasheet field aligned currents and parallel electric fields, 1974.
- 136 - ACKERMAN, M., P. SIMON, U. von ZAHN and U. LAUX, Simultaneous upper air composition measurements by means of UV monochromator and mass spectrometer, 1974.
- 137 - KOCKARTS, G., Neutral atmosphere modeling, 1974.
- 138 - BARLIER, F., P. BAUER, C. JAECK, G. THUILLIER and G. KOCKARTS, North-South asymmetries in the thermosphere during the last maximum of the solar cycle, 1974.
- 139 - ROTH, M., The effects of field aligned ionization models on the electron densities and total flux tubes contents deduced by the method of whistler analysis, 1974.
- 140 - DA MATA, L., La transition de l'homosphère à l'hétérosphère de l'atmosphère terrestre, 1974.
- 141 - LEMAIRE, J. and R.J. HOCH, Stable auroral red arcs and their importance for the physics of the plasmopause region, 1975.
- 142 - ACKERMAN, M., NO, NO<sub>2</sub> and HNO<sub>3</sub> below 35 km in the atmosphere, 1975.
- 143 - LEMAIRE, J., The mechanisms of formation of the plasmopause, 1975.
- 144 - SCIALOM, G., C. TAIEB and G. KOCKARTS, Daytime valley in the F1 region observed by incoherent scatter, 1975.
- 145 - SIMON, P., Nouvelles mesures de l'ultraviolet solaire dans la stratosphère, 1975.
- 146 - BRASSEUR, G. et M. BERTIN, Un modèle bi-dimensionnel de la stratosphère, 1975.

- 147 - LEMAIRE, J. et M. SCHERER, Contribution à l'étude des ions dans l'ionosphère polaire, 1975.
- 148 - DEBEHOGNE, H. et E. VAN HEMELRIJCK, Etude par étoiles-tests de la réduction des clichés pris au moyen de la caméra de triangulation IAS, 1975.
- 149 - DEBEHOGNE, H. et E. VAN HEMELRIJCK, Méthode des moindres carrés appliquée à la réduction des clichés astrométriques, 1975.
- 150 - DEBEHOGNE, H. et E. VAN HEMELRIJCK, Contribution au problème de l'aberration différentielle, 1975.
- 151 - MULLER, C. and A.J. SAUVAL, The CO fundamental bands in the solar spectrum, 1975.
- 152 - VERCHEVAL, J., Un effet géomagnétique dans la thermosphère moyenne, 1975.
- 153 - AMAYENC, P., D. ALCAYDE and G. KOCKARTS, Solar extreme ultraviolet heating and dynamical processes in the mid-latitude-thermosphere, 1975.
- 154 - ARIJS, E. and D. NEVEJANS, A programmable control unit for a balloon borne quadrupole mass spectrometer, 1975.
- 155 - VERCHEVAL, J., Variations of exospheric temperature and atmospheric composition between 150 and 1100 km in relation to the semi-annual effect, 1975.
- 156 - NICOLET, M., Stratospheric Ozone : An introduction to its study, 1975.
- 157 - WEILL, G., J. CHRISTOPHE, C. LIPPENS, M. ACKERMAN and Y. SAHAI, Stratospheric balloon observations of the southern intertropical arc of airglow in the southern american aera, 1976.
- 158 - ACKERMAN, M., D. FRIMOUT, M. GOTTIGNIES, C. MULLER, Stratospheric HCl from infrared spectra, 1976.
- 159 - NICOLET, M., Conscience scientifique face à l'environnement atmosphérique, 1976.
- 160 - KOCKARTS, G., Absorption and photodissociation in the Schumann-Runge bands of molecular oxygen in the terrestrial atmosphere, 1976.
- 161 - LEMAIRE, J., Steady state plasmopause positions deduced from McIlwain's electric field models, 1976.
- 162 - ROTH, M., The plasmopause as a plasma sheath : A minimum thickness, 1976.
- 163 - FRIMOUT, D., C. LIPPENS, P.C. SIMON, E. VAN HEMELRIJCK, E. VAN RANSBEECK et A. REHRI, Lâchers de monoxyde d'azote entre 80 et 105 km d'altitude. Description des charges utiles et des moyens d'observation, 1976.
- 164 - LEMAIRE, J. and L.F. BURLAGA, Diamagnetic boundary layers : a kinetic theory, 1976.
- 165 - TURNER, J.M., L.F. BURLAGA, N.F. NESS and J. LEMAIRE, Magnetic holes in the solar wind, 1976.
- 166 - LEMAIRE, J. and M. ROTH, Penetration of solar wind plasma elements into the magnetosphere, 1976.
- 167 - VAN HEMELRIJCK, E. et H. DEBEHOGNE, Réduction de clichés de champs stellaires pris par télévision avec intensificateur d'image, 1976.
- 168 - BRASSEUR, G. and J. LEMAIRE, Fitting of hydrodynamic and kinetic solar wind models, 1976.
- 169 - LEMAIRE, J. and M. SCHERER, Field aligned distribution of plasma mantle and ionospheric plasmas, 1976.
- 170 - ROTH, M., Structure of tangential discontinuities at the magnetopause : the nose of the magnetopause, 1976.
- 171 - DEBEHOGNE, H., C. LIPPENS, E. VAN HEMELRIJCK et E. VAN RANSBEECK, La caméra de triangulation de l'IAS, 1976.
- 172 - LEMAIRE, J., Rotating ion-exospheres, 1976.
- 173 - BRASSEUR, G., L'action des oxydes d'azote sur l'ozone dans la stratosphère, 1976.
- 174 - MULLER, C., Détermination de l'abondance de constituants minoritaires de la stratosphère par spectrométrie d'absorption infrarouge, 1976.
- 175 - VANCLOOSTER, R., First and second order approximation of the first adiabatic invariant for a charged particle interacting with a linearly polarized hydromagnetic plane wave, 1976.
- 176 - VERCHEVAL, J., Détermination des conditions de lancement de Spacelab en vue de rencontrer les exigences d'un projet d'expérience par spectrométrie d'absorption, 1977.
- 177 - LEMAIRE, J., Impulsive penetration of filamentary plasma elements into the magnetospheres of the Earth and Jupiter, 1977.
- 178 - SIMON, P.C. and D. SAMAIN, Solar flux determination in the spectral range 150-210 nm, 1977.
- 179 - SIMON, P.C., Le rayonnement ultraviolet du soleil et ses relations avec l'aéronomie, 1977.